Nguyen Thi Mai

Study on the geometrical and electronic structures of cluster atoms doping transition metals using quantum calculation approach for orientation of application in catalytic materials

Major: Electronic Material
Code: 9440123

SUMMARY OF MATERIAL SCIENCE DOCTORAL THESIS

Ha Noi - 2023

ABSTRACT

In the advanced material science field, artificial atomic clusters with sub-nanometer structures have recently been of particular interest to scientists. At sizes ranging from a few to a few tens of atoms, the properties of atomic clusters vary interestingly and are difficult to predict due to the impact of quantum effects. The geometrical and electronic structures of atomic clusters change anomalously when just one atom is added or removed. Therefore, the atomic clusters have recieved much attention with the aim to look for and create stable atomic clusters like a super atom with properties that can replace or exceed those of other elements in the Periodic Table, as a building block for the development of new advanced nanomaterials. Recent research results have shown that adding/doping transition metals can change the stability of the atomic clusters, enhance the magnetic properties, optical properties or change the desired catalytic activity. In which, the transition metal atoms with single electrons on the d orbital play a key role, participating in adjusting the geometric structure and electronic structure of the atomic cluster. The combination between transition metal atoms and atoms of other elements in an atomic cluster can change the catalytic activity, magnetic moment, optical absorption properties, bandgap size, or chemisorption while preserving the stability of the atomic clusters. Semiconductor elements are an important material in the electronics industry and have been deeply and extensively integrated in the modern and advanced manufacturing industry. Studying the atomic clusters of semiconductor elements doped with transition metal atoms is expected to modify the physicochemical properties of semiconductor materials at the atomic and molecular level, thereby finding new properties and then applying in the semiconductor industry. Not only with semiconductor elements, the atomic clusters of precious metals and transition metals are considered as an ideal fundamental research model to clarify the question of whether or not the formation of the Kondo effect is at the smallest structure level. In this model, the valence electrons in the noble metal atoms form free electron cloud while the localized electrons in the d-orbital of the transition metal atom are considered as a single magnetic moment co-existing at the atomic or molecular level. Changing the number of noble metal atoms and appropriately choosing the transition metal allows to adjust the finite size of the free electron cloud and the magnitude of the magnetic moment, thereby observing the formation and magnetic quenching of impurities in the atomic cluster structure. Oxide atom Clusters of transition metals are also an interesting object. In bulk

form, transition metal oxides have a wide range of magnetic, optical, and electrical properties and have various applications in the fields of electronics, catalysis, and energy. Despite following the fundamental rules, the physical and chemical properties of transition metal oxide clusters vary anomalously in term of the size and composition, and uven though can have properties that are in superiority over those of their bulk form.

So far, the understanding about atomic clusters containing transition metals is still unclear. The research process approaching by quantum computing methods faces many difficulties due to the appearance of d-shell electrons in transition metal atoms, leading to a large number of structural isomers. They have different electronic configurations but have similar energy levels. Along with that, there are many unanswered questions about the rule of structural change as well as the complex interactions between d-localized electrons of transition metal atoms and free electrons belonging to the electron shell of the atom cluster. These electronic interactions are the prerequisites for the interesting catalytic, magnetic, and optical properties of the atomic cluster. Therefore, we selected the topic "Study on the geometrical and electronic structure of the transition metal atom cluster by quantum computing method for applying orientation in the field of catalytic materials". This dissertation focuses on three main research objects, namely atomic clusters of semiconductor elements and transition metals, oxide atom clusters of transition metals and atomic clusters of precious metals and transition metals.

The target of dissertation

The research objective of the dissertation is to clarify the stable geometric structure, build the electronic structure, dissociation mechanism, existence rule and the change of the valence electrons of atomic clusters, that are atomic cluster of semiconductor element and transition metals, oxide atomic clusters of transition metals and atomic clusters of noble metals and transition metals. Based on the results, we design and propose stable atomic clusters with special properties such as "superatoms" for the fabrication of new nanomaterials in the future.

The main content of dissertation

The geometrical and electronic structure of the atomic cluster of the silicon element and the transition metal $Si_nMn_2^+$ (n = 1-10) and the oxide atom cluster of the transition metal $Co_nO_m^+$, and atomic clusters of precious and transition metals

$Au_{19}TM$ (TM = Sc, Ti, V, Cr, Mn, Fe, Co, Ni and Cu) and CrM_n (n = 2-20, M = Cu, Ag, Au) are determined.

Clarifying the process of electronic interaction as well as the co-existence of filled electron shells and local unpaired electrons in the studied atom clusters.

Determining the stability and clarifying the photodissociation mechanism of the atomic clusters and comparing with some experimental results.

Determining the correlation between the geometric structure, valence electrons of each atom, and the law of filling the electronic shells of the atomic clusters.

Dissertation layout

In addition to the introduction, conclusion and references, the content of the thesis is presented in 5 chapters. Chapter 1 introduces an overview of the research field, Chapter 2 reviews the theoretical foundation and research methods, the last three chapters present the results and discussion. The titles of the chapters are as follows:

Chapter 1. Overview of transition metal atom clusters.

Chapter 2. Theories and research methods.

Chapter 3. Atomic clusters of transition metals and silicon $Si_nMn_2^+$.

Chapter 4. Atomic clusters of transition metal oxides $Co_nO_m^+$.

Chapter 5. Atomic clusters of transition metals and noble metals $Au_{19}TM$, CrM_n.

The main results of the dissertation have been published in 08 specialized articles, including: 04 articles published in international journals on the list of ISI, 04 articles published in nation journals.

CHAPTER 1. OVERVIEW OF TRANSITION METAL ATOMIC CLUSTERS

1.1. Introduction on atomic clusters

The properties of macroscopic materials are usually independent on the size of the material. However, in the world of extremely small atomic clusters, the picture of the properties of materials is not only radically different, but also very interesting. Atomic clusters are collections of a few to several dozen atoms bonded together in a close order and it is, ideally, unaffected by external interactions, forming nanometer-sized structures (nm) or less. Due to the large number of atoms on the surface and the quantum size effect, the geometric structure, physical

properties, and chemical properties of clusters of atoms, are often completely different from the crystal structure in the form of its own crystal blocks, which can change suddenly when their size is changed. Therefore, the atomic clusters attract the interest of scientists not only because of the desire to expand the fundamental understanding about the change of physicochemical properties of matter from an atom bulk materials, but also by the expectation of using smaller but smarter material structures for technological applications. During the bonding process, the valence electrons in each atom can move freely to another atom and form a common electron shell of the whole atomic cluster with different energy levels which differ from the electron shell of the atom. While the properties of elements in their monatomic and bulk forms, respectively, have been studied and clarified, the physical and chemical properties of atomic clusters are difficult to predict. Adding or subtracting just one atom drastically alters the geometry and electronic structure of these clusters, giving rise to anomalous optical, electronic, and magnetic properties that we have never observed before. In the field of catalysis, the atomic clusters become even more special due to their large surface area to volume ratio. Each the atomic cluster can then act as an artificial catalytic system in the catalysis process. The selectivity and catalytic activity of the atomic clusters are expected to be modified by integrating new catalytic sites, changing the charge distribution, and controlling the number of atoms and their structure.
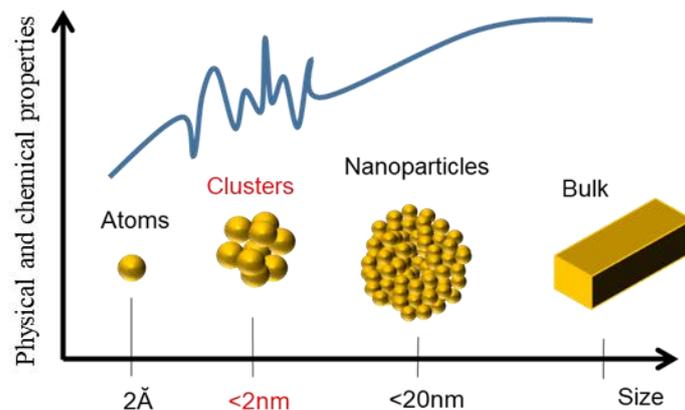
Figure 1.1. The property modification of atom in term of the size.

Doping is one of the effective approaches to modify the properties of atomic clusters. Recent researches have shown that the interaction between the valence electrons of the transition metal atom and the electronic shell structure of the doped atomic cluster is the main cause of the change in the stability of the atomic cluster, enhance the magnetic, optical properties or modify the catalytic activity as desired. The heterojunction between the atom of the doped cluster and the

transition metal atom is also a key factor affecting its stable geometric structure. The rule governing the geometrical and electronic structures of the atomic cluster, thereby changing the magnetic moment, optical absorption characteristic, bandgap, or adsorption capacity and catalytic activity that still remains the stability of many complex binary atomic clusters containing transition metals which need to discuss morre. In addition, the appearance of d-shell electrons of these metals creates a lot of degenerate isomers in terms of energy and spin configurations. Just two transition metal atoms lead to a huge number of isomers with nearly the same energy levels. Reliably determining the most stable structure from the number of degenerate isomers is also a big challenge for binary atomic clusters containing transition metals. Even so, these atomic clusters promise extremely interesting physical properties and their potential applications deserve a lot of research attention. Therefore, it is extremely useful when the binary atomic clusters containing transition metals are simulated, modeled, and their properties are reliably predicted, in preparation for experimental studies in the future.

CHAPTER 2. THEORIES AND RESEARCH MODEL

To simulate the physical properties of clusters of transition metal atoms, such as stable state, geometric structure, and magnetic moment, we use computational methods of quantum chemistry. There are many methods to calculate quantum chemistry, typically ab-initio and density functional methods (DFT). There are DFT methods such as: B3LYP, B3P86, B3PW91, PBEPBE, MPW1PW91... These methods have different $E_{xc}\left[\rho\left(\vec{r}\right)\right]$ functions. To evaluate the reliability of the methods, we performed calculations to study some physical properties of small-size transition metal-doped atomic clusters (dimer, diatomic system) by the density function theory with different functions and sets of functions.

In the current work, we study the characteristics of the atomic cluster $Si_nMn_2^+$ (n = 1-10) by the DFT method. Typically, we choose the B3P86 function and set of functions 6-311+G(d). For the cluster $Co_nO_m^+$, the B3LYP with set of functions 6-31+G(d) is used to optimize computational performance. Atomic clusters of noble metal-transition metal are compatible with BP86 with the set of functions cc-pvTZ-pp used for the noble metal atoms Cu, Ag , Au and cc-pvTZ are used for the transition metal atom.

CHƯƠNG 3. ATOMIC CLUSTERS OF TRANSITION METALS AND SILICON $Si_nMn_2^+$

3.1. Geometric structure

The function B3P86 with the set of function 6-311+G(d) is used to optimize the geometry along with the vibration frequency calculations of the atomic clusters $Si_nMn_2^+$. The geometric structure of silicon cations doped with two manganese atoms has the following form: small-sized clusters of $Si_nMn_2^+$ have a flat structure, larger atomic clusters corresponding to two or more silicon atoms have a 3D structure. From the smallest atomic cluster $Si_1Mn_2^+$ to $Si_3Mn_2^+$, the Si atom is added to bond simultaneously with the silicon atoms of the smaller cluster before it and with two manganese atoms, to form the most Si-Si bonds, being a stronger chemical bond than Mn-Si bond. In larger three-dimensional atomic clusters, the number of bonds that a silicon atom makes with neighboring atoms is always more than the number of bonds that a manganese atom can make with neighboring silicon atoms. The manganese atom in these larger clusters is located mainly on the outer side of the Si_n structure and serves as a bridge between two or three silicon atoms to facilitate the donation of electrons to the Si_n cluster.
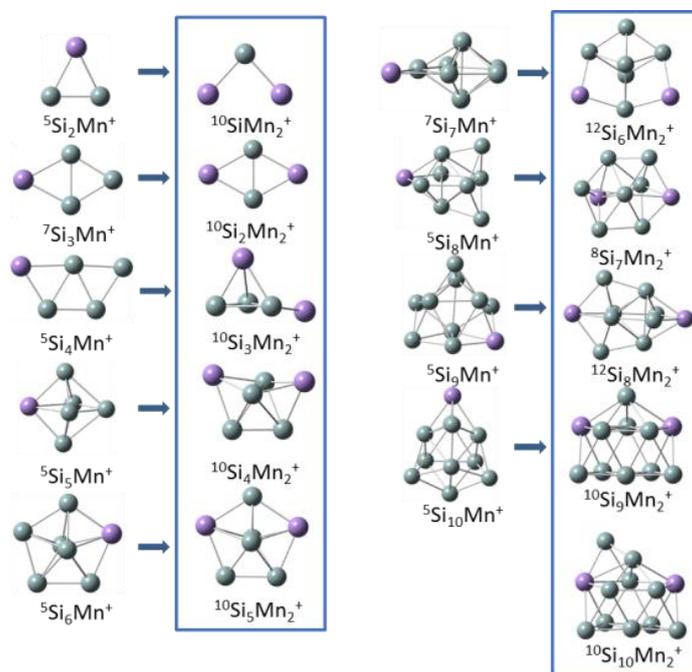
Figure 3.2. The mechanism of growth of the geometrical structure of the atomic cluster $Si_nMn_2^+$ (n = 1-10).

3.2. Electronic structure

The electronic structure of the $Si_nMn_2^+$ (n = 1-10) was specifically determined based on the analysis of the natural binding orbitals and the building of the molecular orbital energy level diagram. The results are presented in Figure 3.3.

It can be seen that all $Si_nMn_2^+$ have a large number of single electrons (from 7 to 9 electrons) located mainly on two Mn atoms depending on the size n. With such electronic configuration, it can be seen that these atomic clusters have catalytic potential with the catalytic center located on two impurity atoms. The electrons $3s^2 3p^2$ of Si atom and $4s^2$ of Mn atom tend to move freely and participate in the formation of the electron shell of the atomic cluster. The $3d^5$ electrons on the two Mn atoms tend to be unpaired and move locally. Except for atomic clusters with n = 1 and 6, the electronic shells of the remaining atomic clusters have the participation of one electron belonging to 3d from the Mn atom.
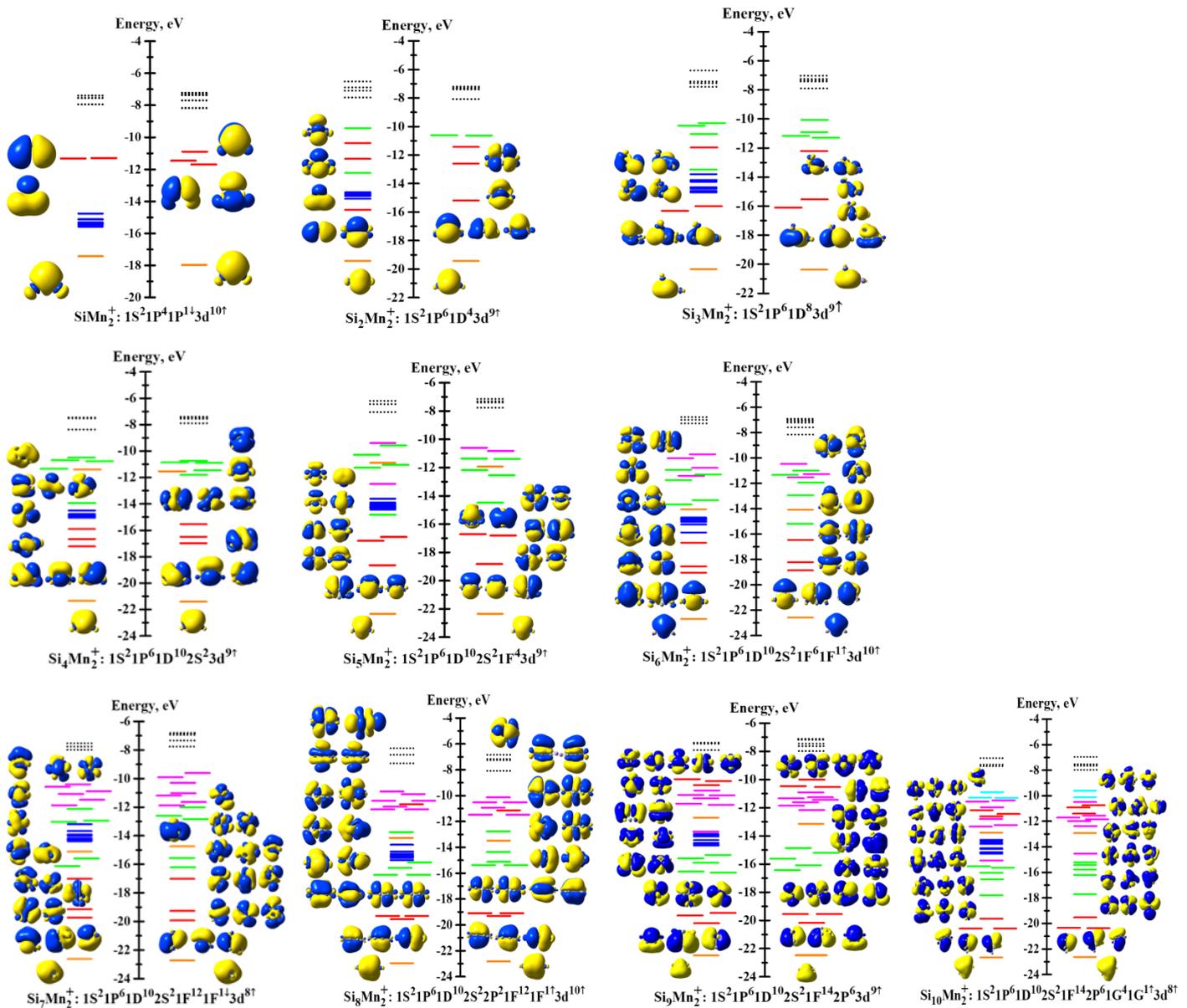
Figure 3.3. Molecular orbital diagrams for $Si_nMn_2^+$ (n = 1-10) with pictures of molecular orbitals.

3.3. Stability and dissociation energy

3.3.1. Average binding energy

The average binding energy BE are determined according to the following formula:

$$BE(Si_nMn_2^+) = \frac{nE(Si) + 2E(Mn^+) - E(Si_nMn_2^+)}{n+2} \qquad (1)$$

$$BE(Si_{n+2}) = \frac{(n+2)E(Si) - E(Si_{n+2})}{n+2} \qquad (2)$$

The average binding energy of the $Si_nMn_2^+$ clusters compared with the pure Si_{n+2} clusters is shown in Figure 3.4. The graph shows that the average binding energy value in the $Si_nMn_2^+$ clusters is larger than that of the pure Si_{n+2} clusters. This proves that the doping of Mn transition metal atoms increases the stability of the $Si_nMn_2^+$. The average binding energy of $Si_nMn_2^+$ is relatively high, from 3.87 eV to 4.21 eV, showing that the studied the $Si_nMn_2^+$ have high stability.
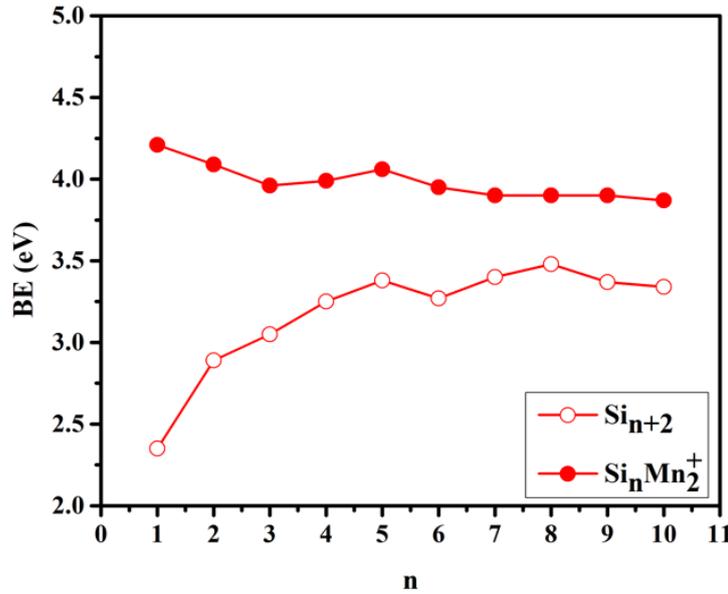
Figure 3.4. Average binding energy BE (eV) of atomic clusters Si_{n+2} và $Si_nMn_2^+$ (n = 1-10)

3.3.2. Second-order difference energy

The relative stability between atomic clusters is analyzed by determining the second-order difference energy (Δ_2E), as follows:

$$\Delta_2E(Si_nMn_2^+) = E(Si_{n+1}Mn_2^+) + E(Si_{n-1}Mn_2^+) - 2E(Si_nMn_2^+) \qquad (3)$$
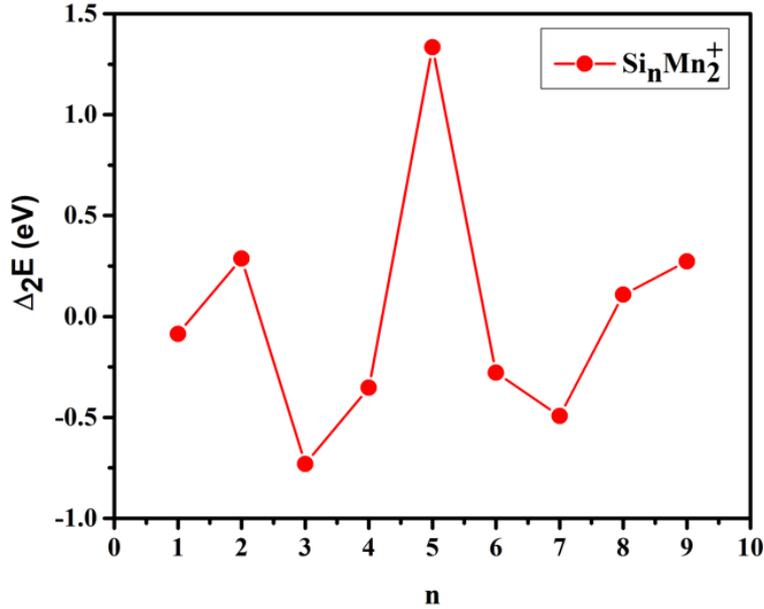
Figure 3.5. Second-order differential energy of atomic clusters $Si_nMn_2^+$ (n = 1-10)

The Δ_2E values are presented in Figure 3.5, it can be seen that the atomic clusters of $Si_2Mn_2^+$, $Si_5Mn_2^+$, $Si_8Mn_2^+$ và $Si_9Mn_2^+$ have higher second-order difference energy than neighboring sizes. It proves that these atomic clusters have a higher stability, this result is consistent with the average binding energy value obtained. In which, the maximum second-order binding energy is obtained at size n = 5 with 1.33 eV, so $Si_5Mn_2^+$ is the atomic cluster with the highest stability compared to the studied sizes.

3.3.3. Dissociation energy

Dissociation energy of the $Si_nMn_2^+$ based on the theoretical level B3P86/6-311+G(d) calculated for dissociation channels. From the obtained results, it can be seen that the $Si_nMn_2^+$ mainly dissociates in two directions to form neutral Mn atom and Mn^+ cation. In which, the atomic clusters $Si_5Mn_2^+$, $Si_8Mn_2^+$ và $Si_9Mn_2^+$ are more stable atomic clusters compared to neighboring sizes. At the same time, we can see that the atomic clusters $Si_6Mn_2^+$, $Si_7Mn_2^+$ và $Si_{10}Mn_2^+$ are unstable because the energy required to trigger their dissociation is lower than that of neighboring clusters.

The results of testing the average binding energy, the difference in second-order binding energy and the dissociation energy show that the atomic clusters $Si_5Mn_2^+$, $Si_8Mn_2^+$ và $Si_9Mn_2^+$ have higher stability than neighboring atomic clusters. It is well suitable for fabrication and synthesis by experimental techniques.

CHƯƠNG 4. ATOMIC CLUSTERS OF TRANSITION METAL OXIDES $Co_nO_m^+$

4.1. Photodissociation experiment of atomic clusters $Co_nO_m^+$ (n = 5-9, n-2 ≤ m ≤ n+2)

The dissociation experiments of cobalt oxide atom cluster were performed by Assoc. Dr. Nguyen Thanh Tung with support of Prof. Dr. Ewald Janssens at the Laboratory of Molecular and Laser Spectroscopy, KU Leuven University, Belgium. The mass-selective mass spectrometer coupled mass spectrometer (MSPFS) dissociation technique is used, as shown in Figure 4.1. In which, cobalt oxide atom cluster are created by evaporating the Co using a 10 Hz pulsed laser at 532 nm and an energy density of about 8-14 mJ/cm^2 simultaneously with the addition of oxygen gas. When fabricating alloy atom clusters, two laser beams are activated simultaneously to evaporating on the surface of two different respective metal substrates. After evaporation, high-temperature atoms, molecules, and ions of random composition and size will be cooled by a stream of carrier gas (usually helium). During the cooling process, these alloy atoms, molecules, and ions increase gradualy in term of time, forming clusters of cobalt oxide atoms. By controlling the carrier gas flow time and pressure, cobalt oxide atom cluster can form with different sizes and oxygen concentrations.
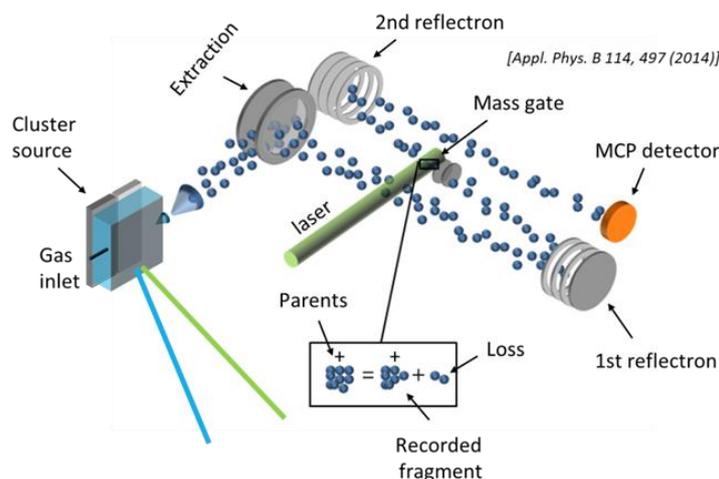
Figure 4.1. Studying the dissociation of atomic clusters by photodissociation technique combined with MSPFS mass spectrometer.

The results obtained are the intensity signals of the parent atom clusters, secondary atomic clusters and their respective flight times in TOF-MS which we analyzed, evaluated and synthesized in Figure 4.2.
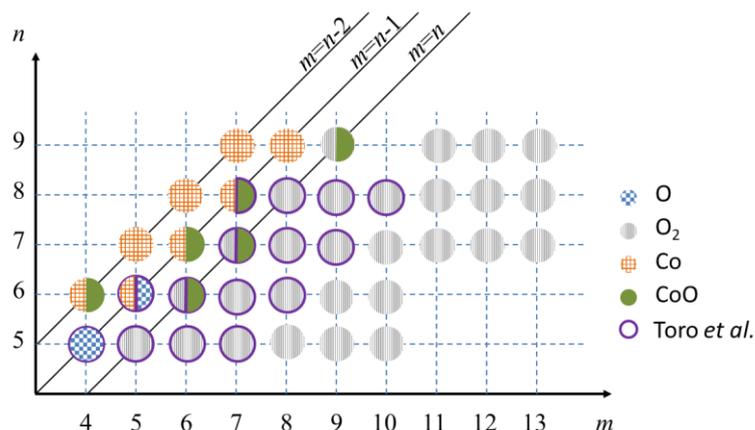
Figure 4.2. Summary of main dissociation channels of $Co_nO_m^+$ (n-2 $\leq$ m $\leq$ n+2). The circles corresponding to the dissociation channels of O, O_2, Co and CoO are denoted on the right. The purple outlines are the results being consistent with the data of Toro et al.

4.2. Geometric structure of $Co_nO_m^+$ clusters

We used the density function B3LYP with the basis set of 6-31+G(d) to optimize the geometry along with the vibration frequency of the $Co_nO_m^+$ clusters.

The pyramid structure is defined for the clusters of $Co_8O_6^+$, $Co_8O_5^+$ and $Co_8O_4^+$, where the O atoms tend to bond to the faces of the Co_8 tower. The clusters of $Co_7O_n^+$ (n = 3-6) and $Co_6O_n^+$ (n = 2-5) are most stable in the form of Co_7 and Co_6 bipyramidal cores, respectively. The first oxygen atoms participate in the bonding with the triangular faces of three Co atoms, while the subsequent atoms occupy the bridging position for the Co-O-Co bond. The geometric structure of the $Co_5O_4^+$ cluster consists of a Co-O-Co bond chain, like a ladder with a frame of $Co_4O_4^+$ molecules and limited by a Co atom. Meanwhile, $Co_5O_3^+$ has the form of a symmetric square pyramid with two O atoms attached to opposite faces and another O atom occupying a Co-O-Co bridge site.

4.3. Electronic structure of $Co_nO_m^+$ clusters

Transition metal atoms with a large number of valence electrons in the d-shell have the ability to interact but are highly local, which hinders the formation of electron shell structures in clusters of transition metal atoms. The results of calculating the electronic structure of the clusters of $Co_nO_m^+$ show a similar picture. The valence electrons on the atoms in this cluster do not move freely to form the common electronic structure of the cluster, but they exist locally on each component atom. Clusters of $Co_nO_m^+$ that are stable at high spin multiples mainly around 13-20, characterized by a large number of single electrons, have the

potential to become materials with strong catalytic activity.

4.4. Dissociation energy of $Co_nO_{n-2}^+$ clusters

From the electronic energy values of the most stable structures optimized, taking into account the corresponding zero-point vibration energies, we calculated the dissociation energies (DE) of the $Co_nO_m^+$ clusters (n = 5 -8, m = n-2) for the selected potential dissociation channels as follows:

(1) $Co_nO_m^+ \rightarrow Co_nO_{m-1}^+ + O$ (2) $Co_nO_m^+ \rightarrow Co_nO_{m-2}^+ + O_2$

(3) $Co_nO_m^+ \rightarrow Co_{n-1}O_m^+ + Co$ (4) $Co_nO_m^+ \rightarrow Co_{n-1}O_{m-1}^+ + CoO$

It can be seen that the $Co_nO_{n-2}^+$ clusters (n = 6-8) have fragmentation into similar channels. The main dissociation direction of these clusters is to cleave a Co atom. Other dissociation channels include the cleavage of one O_2 molecule, one CoO molecule or one O atom. In particular, only 2.3 eV and 3.77 eV are required for the dissociation of $Co_8O_6^+$ and $Co_6O_4^+$, respectively. Meanwhile, at least 4.2 eV is required for the fragmentation of $Co_7O_5^+$. The second preferred dissociation channel that can be seen is the fragmentation of a CoO molecule with the corresponding energy of 2.7 eV; 5.37 eV and 4.37 eV for the $Co_8O_6^+$, $Co_7O_5^+$ and $Co_6O_4^+$ clusters.
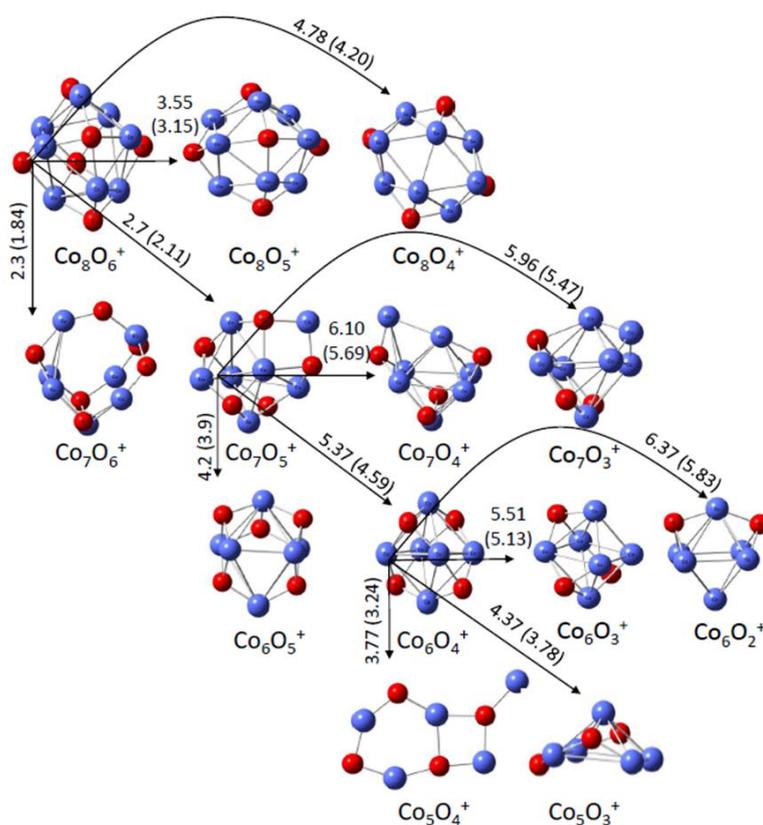
Figure 4.6. Representation of the possible dissociation channels of

$Co_8O_6^+$, $Co_7O_5^+$ và $Co_6O_4^+$ and dissociation energy (eV) corresponding to the evaporation of O, O_2, Co và CoO. The values in parentheses are the results of the Gibbs energy variation calculation ΔG (eV) at 300 ^{0}K.

4.4. Calculation of Gibbs free energy variation of $Co_nO_{n-2}^+$ clusters

Calculation results of thermodynamic variation ΔS according to a number of different atomic and molecular dissociation channels are shown in Table 4.2. It is obvious that the increase in entropy along dissociation channels resulting in the evaporation a molecule (O_2 or CoO) is larger than dissociation channels which evaporates an atom (O or Co). This result is completely consistent with the above discussion. The dissociation channels of CoO molecules of the $Co_nO_m^+$ clusters have a higher thermodynamic increase than the dissociation channels of a Co atom or an O atom at the same analytical temperature. Similarly, channels that dissociate into an O_2 molecule have a higher entropy value than channels that dissociate into an O atom. Thus, if the two channels dissociate into a CoO molecule or a Co atom, they need to have the same dissociation energy value. As a result, the CoO molecular dissociation channel will be preferred because it has a larger value of entropy thermodynamic variation and therefore smaller ΔG.

CHƯƠNG 5. ATOMIC CLUSTERS OF TRANSITION METALS AND NOBLE METALS CrM_n và $Au_{19}TM$

5.1. Atomic clusters of transition metals and noble metals $Au_{19}TM$
5.1.1. Studying the stable geometric structure of the atomic clusters of transition metals and noble metals $Au_{19}TM$ (TM = Sc - Cu)

The stable geometric structure of the $Au_{19}TM$ clusters (TM = Sc − Cu) is determined based on the density functional theory method with the BP86 functional together with the basis set of cc-pVDZ-pp and the set of cc-pVDZ applying to Au atom and 3d transition metal atom, respectively (TM = Sc-Cu).

The stable geometric structure of the clusters of $Au_{19}Sc$ and $Au_{19}Ti$ is nested form, the Sc and Ti atoms substitute for the Au atom in the central position to create the maximum number of coordination with the host atoms of the gold cluster. The $Au_{19}TM$ clusters (TM = Cr-Cu), the geometric structure tends to keep the Au_{20} tetrahedral structure with the doped atoms located at the centers of the faces of the tetrahedron. A structural competition occurs at $Au_{19}V$, the pyramid state seems to be the lowest energy structure but cage and tetrahedral structures with V-doped atom replacing surface-centered Au atom are also found to be very

stable at +0.03 and +0.09 eV, respectively. Thus, the $Au_{19}V$ cluster can be considered as a geometrical transition point, where the structure of the $Au_{19}TM$ clusters begins to change from a nest to a tetrahedral shape.

$Au_{19}Sc$-A	$Au_{19}Sc$-B	$Au_{19}Sc$-C	$Au_{19}Ti$-A	$Au_{19}Ti$-B	$Au_{19}Ti$-C
^{1}0.00	^{1}0.15	^{1}0.16	^{2}0.00	^{2}0.04	^{2}0.07
$Au_{19}V$-A	$Au_{19}V$-B	$Au_{19}V$-C	$Au_{19}Cr$-A	$Au_{19}Cr$-B	$Au_{19}Cr$-C
^{5}0.00	^{3}0.03	^{3}0.07	^{6}0.00	^{5}0.33	^{6}0.48
$Au_{19}Mn$-A	$Au_{19}Mn$-B	$Au_{19}Mn$-C	$Au_{19}Fe$-A	$Au_{19}Fe$-B	$Au_{19}Fe$-C
^{5}0.00	^{5}0.08	^{7}0.14	^{4}0.00	^{4}0.23	^{4}0.29
$Au_{19}Co$-A	$Au_{19}Co$-B	$Au_{19}Co$-B	$Au_{19}Ni$-A	$Au_{19}Ni$-B	$Au_{19}Ni$-C
^{3}0.00	^{3}0.16	^{3}0.40	^{2}0.00	^{2}0.26	^{2}0.32
$Au_{19}Cu$-A	$Au_{19}Cu$-B	$Au_{19}Cu$-C			
^{1}0.00	^{1}0.29	^{1}0.52			
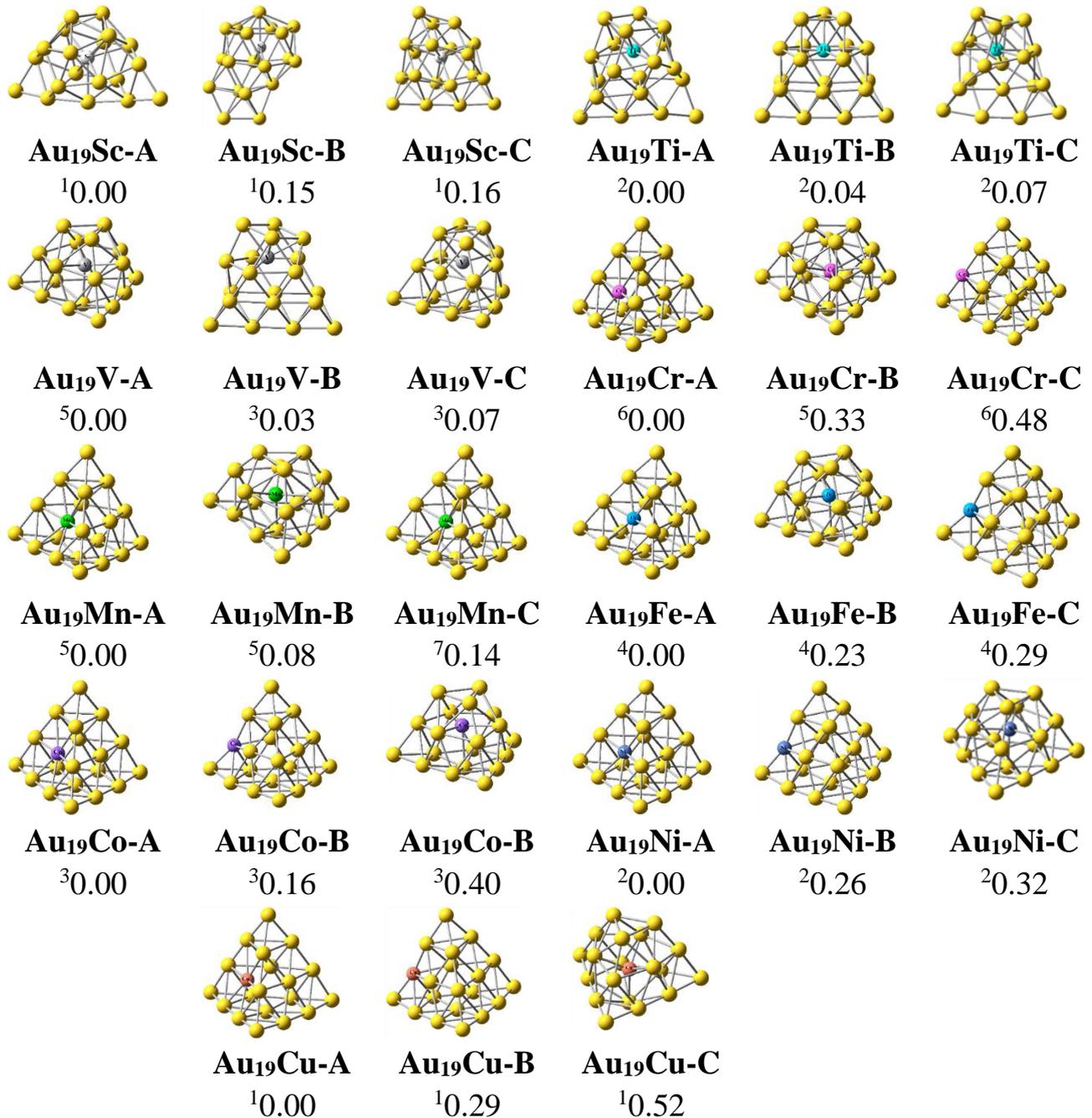
Figure 5.1. Geometric structures, spin coefficients and relative energies (eV) of the most stable isomers for $Au_{19}TM$ (TM = Sc-Cu) clusters.

5.1.2. Electronic structure

Similar to the Au_{20} pyramid, the existence of a fully closed electron shell and obeying the 20-electron rule was observed for $Au_{19}TM$ clusters. With the tetrahedral structure of $Au_{19}TM$ clusters, the energy of the 2S orbitals is strongly reduced, creating a completely occupied electron shell of $1S^21P^62S^21D^{10}$.

Meanwhile, with the spherical cage structure, the $Au_{19}Sc$ and $Au_{19}Ti$ clusters form an electronic structure with energy levels corresponding to the $1S^2 1P^6 1D^{10} 2S^2 1F^2$ configuration.

Notably, $Au_{19}Cr$ has a closed 20-electron structure of $1S^2 1P^6 2S^2 1D^{10}$. It means that this atomic cluster is very stable, co-existence of 5 free electrons evenly distributed into 3d orbitals of Cr atom. Single electrons form the ideal electronic interaction environment for the catalytic properties of the $Au_{19}Cr$ cluster. It can be expected that $Au_{19}Cr$ is a superatom which has a catalytic potential with the catalytic center located on the Cr transition metal atom.
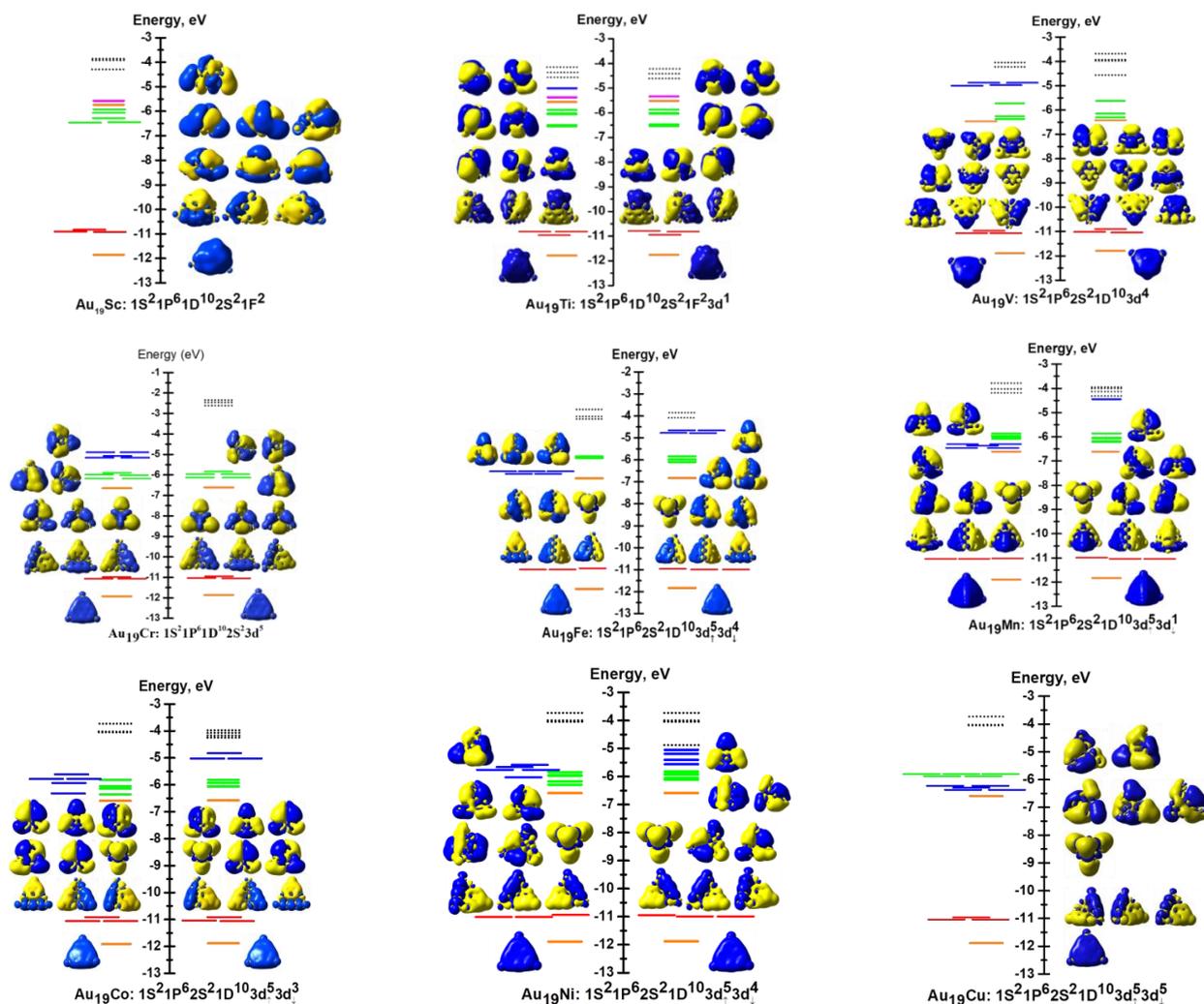
Figure 5.3. Molecular orbital diagrams for $Au_{19}TM$ (TM = Sc-Cu) with images of molecular orbitals.

5.1.3. Stability and dissociation energy

To study the stability of $Au_{19}TM$ clusters, we determined the dissociation energy of $Au_{19}TM$ clusters in the following dissociation directions:

$$Au_{19}TM \rightarrow Au_{19} + TM \quad (1) \qquad\qquad Au_{19}TM \rightarrow Au_{18}TM + Au \quad (2)$$
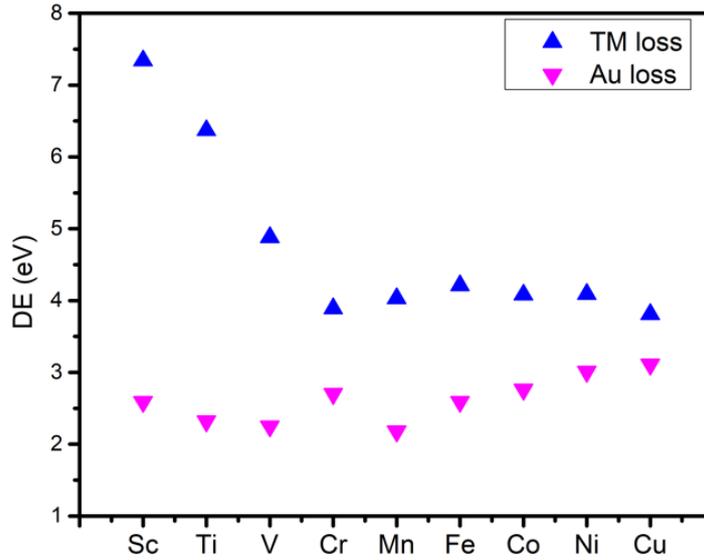
Figure 5.4. Dissociation energy of $Au_{19}TM$ cluster according to different dissociation channels.

It can be seen that for all $Au_{19}TM$ clusters, the evaporation of one Au atom to form $Au_{18}TM$ is the most energetically preferred dissociation channel. Whereas, the $Au_{19}Mn$ cluster has the lowest dissociation energy. The energy required for the $Au_{19}TM$ cluster to dissociate into Au_{19} and a TM atom is relatively large, especially for the Sc, Ti and V doped clusters. The minimum energy to dissociate into the Sc and Ti atom is 7.34 eV and 6.37 eV, respectively. Among the studied clusters, $Au_{19}Cr$, $Au_{19}Co$, $Au_{19}Ni$ and $Au_{19}Cu$ are more stable with the minimum energy required to liberate an Au atom of 2.70; 2.76; 3.01 and 3.11 eV, respectively. The least stable cluster is $Au_{19}Mn$ with 2.18 eV that can dissociate into $Au_{18}Mn$ and one Au atom. The stability of $Au_{19}TM$ clusters can be evaluated based on the bandgap energy (HOMO – LUMO) value, which is calculated as follows:

$$\delta_1 = -(\varepsilon^{\alpha}_{HOMO} - \varepsilon^{\beta}_{LUMO})$$
$$\delta_2 = -(\varepsilon^{\beta}_{HOMO} - \varepsilon^{\alpha}_{LUMO})$$

With a very large HOMO - LUMO bandgap of 1.76 eV and a high dissociation energy value of 3.11 eV, it can be concluded that the $Au_{19}Cu$ tetrahedron is extremely stable and this stability can be compared with the stability of the Au_{20} pyramid. The $Au_{19}Sc$ atomic cluster with a closed electron shell has a smaller HOMO-LUMO bandgap (1.26 eV), but this value is still remarkable, indicating that $Au_{19}Sc$ is more stable and less reactive. The bandgap energies of $Au_{19}Mn$ and $Au_{19}V$ are the smallest (0.26 and 0.30 eV, respectively), indicating that they are

more reactive than the other clusters while $Au_{19}Cr$ is the least reactive to the highest bandgap energy (0.78 eV).

5.2. Atomic cluster of transition metal – noble metal CrM_n

5.2.1. Atomic cluster of transition metal and noble metal CrM_n (M=Cu, Ag, Au, n = 2-20)

We used the density function theory BP86 with the basis set of cc-pVTZ-pp for Cu, Ag, Au atoms and the cc-pVTZ for the Cr atom to optimize the geometry together with oscillation frequency calculations of clusters Cu_nCr, Ag_nCr and Au_nCr. The optimal geometric structure of Cu_nCr, Ag_nCr and Au_nCr clusters is shown in Figure 5.5.
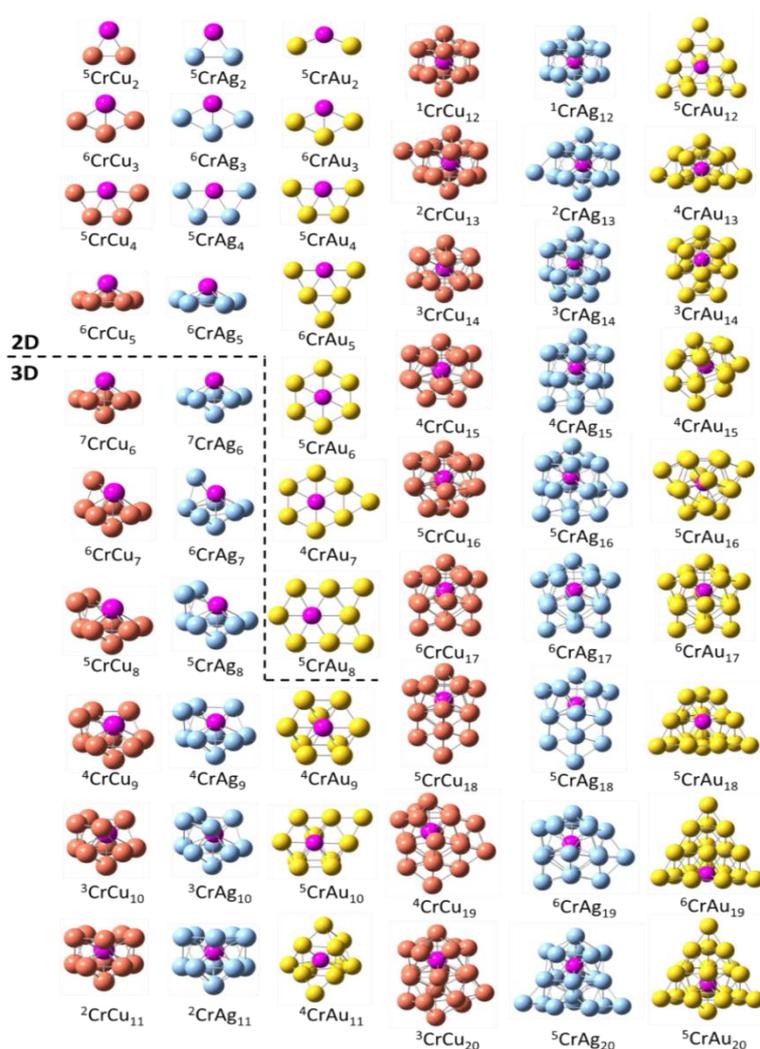
Figure 5.2. Most stable geometries and the corresponding spin multiplicities of CrM_n clusters (M = Cu, Ag, Au, n = 2-20), in which the Cr, Cu, Ag and Au atoms are pink, orange, blue and yellow, respectively.

From the geometrical features described above, we can clearly see the transformation rule of geometric structure of CrM_n clusters. The small sized CrM_n

clusters (n ≤ 5 with M = Cu, Ag and n ≤ 8 with M = Au) favor a planar geometry. Larger clusters tend to form three-dimensional geometrical structures. The Cr atom tends to attach to the sites with the highest coordination number. The tetrahedral structure is believed to be the basic framework for the geometric growth of the $CrAu_n$. The substitution of an Au atom in the Au_{n+1} cluster by a Cr atom to form the $CrAu_n$ complex cluster generally leads to a significant structural rearrangement. Except the clusters with planar structure (n = 2-8), the geometry of the pure Au_{n+1} cluster still remains when replacing one Cr atom. In contrast, at larger sizes, the stable geometry of the doped $CrAu_n$ clusters is completely different from that of the Au_{n+1} clusters. Meanwhile, the atomic clusters $CrCu_n$ and $CrAg_n$ have a geometric growth rule that follows a completely different picture. At size n = 6-12, the geometrical structure grows by the mechanism to form a hexagonal structure from the pentagonal bipyramidal (n = 6). The geometric structure evolution of $CrCu_n$ and $CrAg_n$ clusters at larger sizes is based on the tetrahedral framework.

5.2.2. Electronic structure
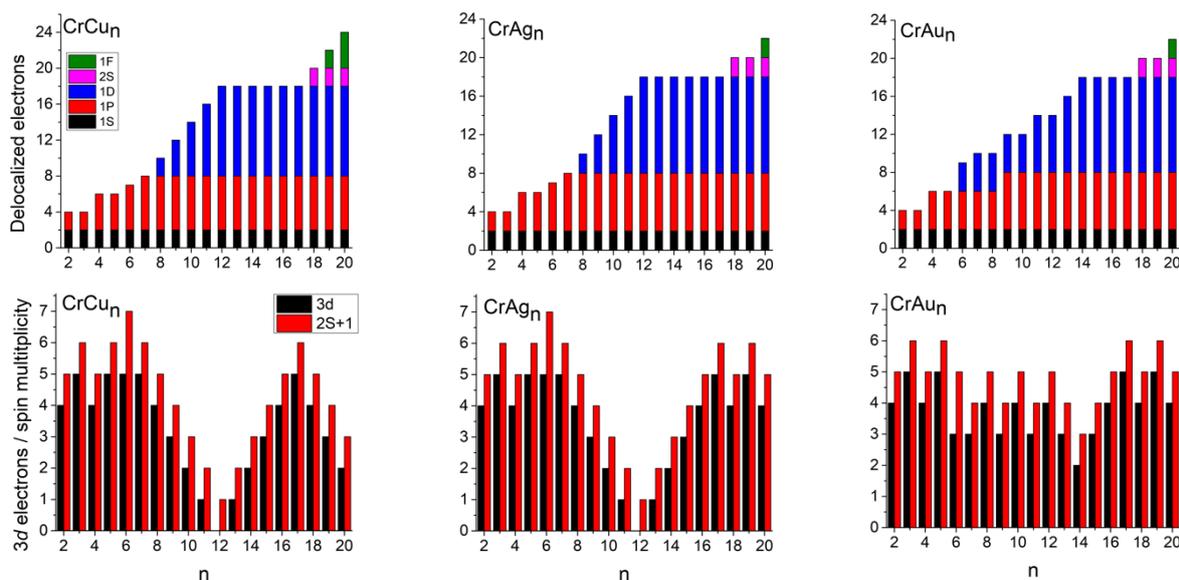
Figure 5.6. Electronic shell fillings, occupations of the localized 3d-Cr orbitals and spin multiplicities for $CrCu_n$, $CrAg_n$ and $CrAu_n$ (n = 2-20).

Figure 5.6 shows the spin states of $CrCu_n$, $CrAg_n$ and $CrAu_n$ clusters at different sizes. The results show that the spin multiples of $CrCu_n$ and $CrAg_n$ clusters at the same size vary almost the same. In which clusters have the spin multiples with two states 5 and 6 in clusters of small size (n ≤ 5). The number of unpaired electrons of the $CrCu_n$ and $CrAg_n$ clusters decreases from 6 to 0 when the size n increases from 6 to 12, then they increase again from 0 to 5 as the size n

increases from 12 to 17 atoms. At the size of 17 to 20, the number of single electrons remaining on the 3d orbital of the Cr atom ranges from 2 to 5 electrons. The valence electrons on the *s-Cr, d*-Cr and *s*-Cu, s-Ag, s-Au orbitals hybridize to form electronic configurations of $CrCu_n$, $CrAg_n$ and $CrAu_n$ clusters with electronic states of position delimiter. These split states lead to the formation of filled electronic shells of atomic clusters, and unpaired localized electrons on the d orbitals. It can be seen in the rule of formation and development of electronic structure of CrM_n clusters, valence electrons $4s^1$, $5s^1$ and $6s^1$ of noble metal atoms (corresponding to Cu, Ag, and Au) and $4s^1$ of the Cr atom tend to move freely, participating in the formation of the electronic shell of the atomic cluster. The numerical contribution of 3d-Cr electrons to the free electron shell of an atomic cluster depends on the cluster size. The remaining 3d electrons on the Cr atom tend to be unpaired and move locally. With the electronic configuration containing simultaneously single electrons on such transition metal atom, it can be seen that these atomic clusters have catalytic potential and the catalytic center is located on the Cr transition metal atom.

5.2.3. Stability and dissociation energy

5.2.3.1. Average binding energy

To understand the influence of Cr doping on the stability of M_nCr alloy clusters (M = Cu, Ag, Au, and n = 2-20), we first conduct average binding energy analysis per atom (*BE*) of the M_nCr and M_{n+1} clusters. The average binding energy value *BE* is determined according to the following formula:

$$BE(CrM_n) = \frac{1}{n+1}[(E(Cr) + nE(M)) - E(CrM_n)] \qquad (1)$$

$$BE(M_{n+1}) = \frac{1}{n+1}[(n+1)E(M)) - E(M_{n+1})] \qquad (2)$$

The average binding energies per atom for the most stable M_{n+1} and M_nCr clusters are presented in Figure 5.9.

The average binding energy analysis results in Figure 5.9 clearly show that *BE* of the M_nCr cluster is a first-order covariate function of the cluster size. The average binding energy of Cu_nCr clusters undergoes two transitions. At small size (n ≤ 7) *BE* of Cu_nCr is smaller than that of Cu_{n+1}. The *BE* transition of the Cu_nCr occurs at size n = 8, the average binding energy of Cu_nCr is significantly higher than that of Cu_{n+1} at n = 8-16, especially at size n = 12. With larger clusters, the difference *BE* between Cu_{n+1} and Cu_nCr is negligible. A similar trend is also observed for Ag_nCr clusters, specifically the *BE* energy transition also takes place at the size n = 8. The replacement of a Cu or Ag atom by a Cr atom causes structural change of Cu_n and Ag_n clusters, the evolutional diagram of Cu_nCr and

Ag$_n$Cr clusters (Figure 5.5) shows the formation of a hexagonal structure at n = 12, which is also the central core of larger clusters.
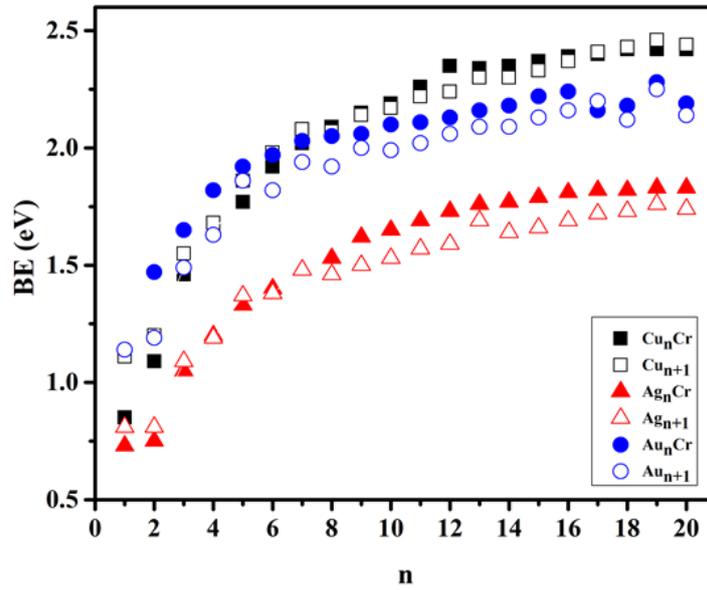
Figure 5.9. Average binding energy of M$_n$Cr và M$_{n+1}$ clusters.

Unlike the Cu$_n$Cr and Ag$_n$Cr clusters, most of the average binding energies *BE* of Au$_n$Cr are larger than the average binding energies of Au$_{n+1}$ (except for the Au$_{17}$Cr). It shows that replacing an Au atom in the Au$_n$ cluster by a Cr atom can enhance the stability of pure Au cluster. It is noteworthy that both Au$_{19}$Cr and Au$_{20}$ clusters have the highest average binding energy values *BE* compared to neighboring sizes, and the energy difference is not significant between these two molecules, leading to the relatively high stability of the tetrahedron with 20 noble metal atoms.

5.2.3.2. Second-order difference energy

The relative stability between atomic clusters is analyzed by determining the second-order difference energy (Δ_2E), as follows:

$$\Delta_2E(CrM_n) = E(CrM_{n+1}) + E(CrM_{n-1}) - 2E(CrM_n) \qquad (3)$$

The calculation results of Δ_2E value shown in Figure 5.10 indicate that for Cu$_n$Cr clusters, the largest difference energy value is determined at size n = 12 with Δ_2E = 1.16 eV, this result is very good consistent with the high stability of the Cu$_{12}$Cr compared with neighboring clusters. The energy difference peak of the Ag$_n$Cr found at n = 9 has a value of Δ_2E = 0.6 eV, which indicates that the Ag$_9$Cr cluster is more stable than that of other sizes. Except the Ag$_2$Cr with the smallest Δ_2E value, the second-order energy difference of other atomic clusters is almost unchanged. For the Au$_n$Cr cluster, the second-order energy difference peak is

determined at n = 19 with $\Delta_2E = 1.02$ eV, indicating that the $Au_{19}Cr$ atomic cluster is the most stable compared to the other sizes.
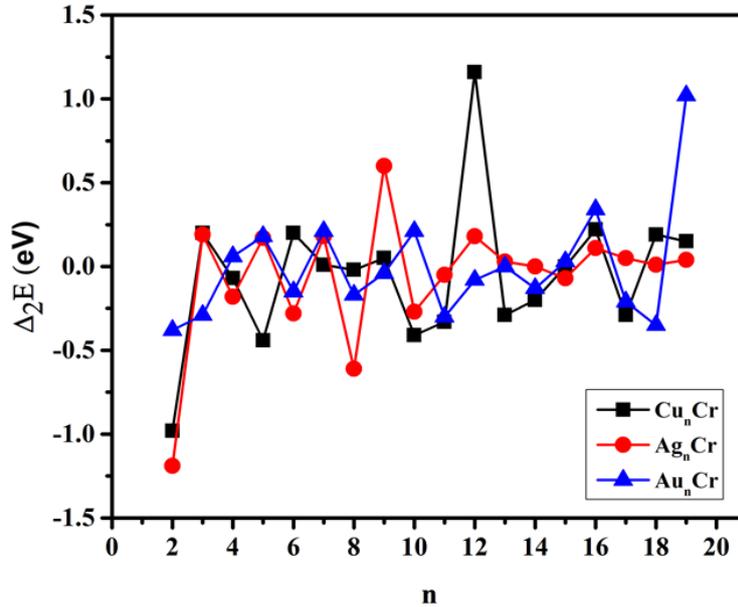
Hình 5.10. Second-order differential energy of M_nCr.

5.2.3.3. Dissociation energy

From the electronic energy values of the most stable structures optimized of the atomic clusters, taking into account the corresponding zero-point vibrational energies, we calculate the dissociation energies (DE) of the clusters studied into smaller clusters according to the following possible dissociation channels:

$$(1)\ M_nCr \rightarrow M_n + Cr \qquad\qquad (2)\ M_nCr \rightarrow M_{n-1}Cr + M$$

The research results show that the tendency to dissociate into a Cr atom is the most obvious dissociation channel for clusters of Cu_nCr atoms at size $n \leq 8$. At larger sizes, the dissociation of Cu atom is energetically preferred up to the size n = 17. The clusters of $Cu_{18}Cr$, $Cu_{19}Cr$ and $Cu_{20}Cr$ give priority to separate a Cr atom. The $Cu_{12}Cr$ dodecahedron exhibits superiority over others because it requires at least 3.37 eV to split a Cu atom or 3.88 eV to release a Cr atom. Compared with Cu_nCr, Ag_nCr clusters tend to dissociate into one Cr atom at size n ≤ 8 and one Ag atom from size n = 9. In which, $CrAg_2$ and $CrAg_6$ are the least stable clusters, only 0.62 and 1.59 eV can dissociate into Ag_2 and Ag_6, respectively. Calculation results of dissociation energy indicate that $CrAg_9$ is the most stable. The minimum energy to break this cluster is 2.58 eV, which is even higher than the energy of the $Ag_{12}Cr$ hexadecimal (2.30 eV). This result is consistent with the calculation result of second-order binding energy difference.
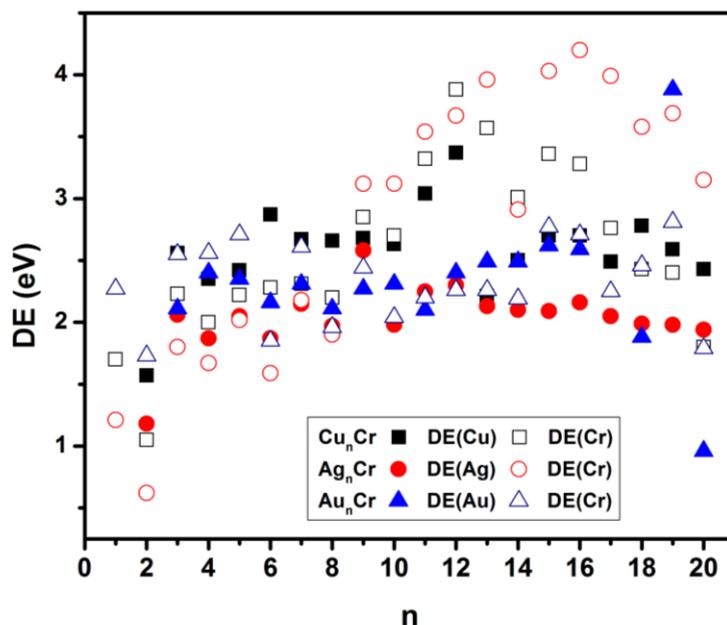
Figure 5.11. Dissociation energy via channels of M_nCr.

Unlike the Cu_nCr and Ag_nCr clusters, the dissociation tendency of Au_nCr clusters is highly dependent on the cluster size. The stability of $Au_{19}Cr$ cluster is the highest, as it requires at least 3.88 and 2.81 eV to separate a Cr atom or an Au atom, respectively, from the cluster. At the same time, it can be seen that the formation of the $Au_{19}Cr$ cluster is quite simple, because only 0.96 eV, the $Au_{20}Cr$ molecule can fragment into the stable $Au_{19}Cr$ and one Au atom.

CONCLUSION

The density functional theory with appropriate sets of basis functions was used in order to study atomic clusters containing transition metals. The main results of the thesis are enumerated below:

1. We have systematically and selectively studied the geometrical structure, stability and electronic structure of atomic clusters of transition metals and elements with different physicochemical properties, which are: i) atomic cluster of transition metal and semiconductor $Si_nMn_2^+$; ii) oxide atom cluster of transition metal $Co_nO_m^+$; and iii) atomic cluster of transition metal and noble metals CrM_n and $Au_{19}TM$ (n = 2-20, M = Cu, Ag, Au and TM = Sc − Cu).

2. In terms of geometric structure, the atomic clusters of transition metals change from 2D to 3D with the increasing of the size. The transformation from 2D to 3D of the $Si_nMn_2^+$ (n = 3) occurs earlier than that of the CrM_n (n = 7). In the atomic cluster of $Si_nMn_2^+$, the transition metal atom is mainly located on the outer

side of the Si_n structure and acts as a bridge between two or three silicon atoms to facilitate the conceding of the electrons to silicon clusters. In contrast, for the CrM_n clusters, the transition metal atom is initially located on the outside and then gradually moves inside the structure of the noble metal cluster to maximize the number of heterojunctions. Meanwhile, the $Co_nO_m^+$ cluster tends to form a [-Co-O-]$_n$ framework attached to over-saturated oxygen atoms/molecules.

3. There is formation of electronic structure in the atomic clusters of $Si_nMn_2^+$, CrM_n and $Au_{19}TM$. Regarding the electronic structure, while the oxide atom cluster of $Co_nO_m^+$ does not form an electronic structure, most of $Si_nMn_2^+$ atomic clusters are stable at high spin multiples, around 8-12 with many free electrons localized on the transition metal atom. The electronic structure of CrM_n and $Au_{19}TM$ has a rule change systematically. Similar to the atomic cluster of $Si_nMn_2^+$, the free electrons are predominantly located in the 3d orbitals of the transition metal atoms.

4. The results of average binding energy, second order bond energy difference and dissociation energy showed that some atomic clusters are more stable than neighboring atomic clusters, being very suitable for synthesizing by experimental techniques, that is $Si_5Mn_2^+$, $Si_8Mn_2^+$ và $Si_9Mn_2^+$, $CrAg_9$, $CrCu_{12}$ and $CrAu_{19}$.

5. The thermodynamic nature of the dissociation process for clusters of $Co_nO_m^+$ was analyzed and clarified. Thermodynamic parameters such as dissociation energy, entropy gradient, Gibbs free energy gradient were determined and compared with the experimental photodissociation results of these atomic clusters. The obtained theoretical calculations are in full agreement with the experimental observations.

6. $Cu_{12}Cr$ and $Au_{19}Cr$ are two clusters with a particularly stable filled electronic structure, which have the potential to become superatoms that can be fabricated and synthesized by physical and chemical methods such as C_{60} fullerence. Notably, $Au_{19}Cr$, in addiction to the filled electronic structure, there is existence in parallel with 5 single electrons evenly distributed in the 3d orbitals of the Cr atom. These single electrons are the ideal electron interaction environment for the interesting catalytic and magnetic properties of the $Au_{19}Cr$ atomic cluster.

NOVEL CONTRIBUTIONS OF DISSERTATION

- The dissertation has indicated the geometrical structure and electronic structure of the atomic cluster of the semiconductor element and the transition metal $Si_nMn_2^+$ (n = 1-10), the oxide atomic cluster of the transition metal $Co_nO_m^+$,

clusters of noble metal and transition metals CrM_n (n = 2-20, M = Cu, Ag, Au) and $Au_{19}TM$ (TM = Sc, Ti, V, Cr, Mn, Fe, Co, Ni and Cu).

- Electronic interaction as well as the co-existence of filled electron shells and local unpaired electrons in the transition metal atomic clusters was clarified.

- The dissertation determined the stability, clarified the photodissociation mechanism of the atomic clusters and compared with some experimental results.

- The correlation between the geometric structure, valence electrons of each atom, and the law of filling the electronic shells of the clusters was characterized.

- More remarkably, the dissertation theoretically predicted that $Au_{19}Cr$ containing 5 unpaired electrons has acted as a "super atom" with strong activities.

DANH MỤC CÁC CÔNG TRÌNH ĐÃ CÔNG BỐ

1. **Nguyen Thi Mai**, Nguyen Thanh Tung, Phan Thi Thuy, Nguyen Thi Minh Hue, Ngo Tuan Cuong, "*A theoretical investigation on $Si_nMn_2^+$ Clusters (n = 1–10): Geometry, stability, and magnetic properties*", Computational and Theoretical Chemistry, **2017**, 1117, 124-129.

2. Nguyen Minh Tam, **Nguyen Thi Mai**, Hung Tan Pham, Ngo Tuan Cuong, and Nguyen Thanh Tung, "*Ultimate Manipulation of Magnetic Moments in the Golden Tetrahedron Au_{20} with a Substitutional 3d Impurity*", Physical Chemistry C, **2018**, 122, 28, 16256-16264.

3. **Nguyen Thi Mai**, Son Tung Ngo, Peter Lievens, Ewald Janssens, and Nguyen Thanh Tung, "*Photofragmentation Patterns of Cobalt Oxide Cations $Co_nO_m^+$ (n = 5-9, m = 4-13): From Oxygen-Deficient to Oxygen-Rich Species*", Physical Chemistry A, **2020**, 124, 7333-7339.

4. **Nguyen Thi Mai**, Ngo Thi Lan, Ngo Tuan Cuong, Nguyen Minh Tam, Son Tung Ngo, Thu Thi Phung, Nguyen Van Dang, and Nguyen Thanh Tung, "*Systematic Investigation of the Structure, Stability, and Spin Magnetic Moment of CrM_n Clusters (M = Cu, Ag, Au, and n = 2-20) by DFT Calculations*", ACS Omega, **2021**, 6, 31, 20341-20350.

5. **Nguyen Thi Mai**, Ngo Thi Lan, Nguyen Thanh Tung, "*Insights into the magnetic origin of Cu_nCr (n = 9÷11) clusters: A superposition of magnetic and electronic shells*", Tạp chí Khoa học và Công nghệ, **2020**, 58, 1, 31-38.

6. **Nguyen Thi Mai**, Nguyen Thanh Tung, Ngo Tuan Cuong, "*Stability and magnetic properties of isomorphous substituted $Si_{7-x}Mn_x^+$*", Tạp chí Khoa học và Công nghệ, **2018**, 56, 1, 64-70.

7. **Nguyen Thi Mai**, Ngo Tuan Cuong, Nguyen Thanh Tung, "*A theoretical investigation on vibrational infrared spectra of $Si_nMn_2^+$ atomic clusters (n = 5-9)*", Tạp chí Khoa học và Công nghệ, **2018**, 56, 1, 33-40.

8. **Nguyễn Thị Mai**, Ngô Tuấn Cường, "*Cấu trúc hình học và các quá trình phân li của cluster silicon Si_n và Si_n^+ (n = 2-10): Một nghiên cứu lý thuyết*", Tạp chí Nghiên cứu Khoa học và Công nghệ quân sự, **2017**, 51.